1998

Quartzite Fabric Transition in a Cordilleran Metamorphic Core Complex

Allen J. McGrew
University of Dayton, amcgrew1@udayton.edu

Martin Casey
University of Leeds

ALLEN J. McGREW AND MARTIN CASEY

Photomicrographs 143A–143F record fabric variations in quartzite with increasing structural depth in a >1 km thick, amphibolite-facies, normal-sense shear zone in the East Humboldt metamorphic core complex, Nevada (Figure 143.1). This shear zone and the overlying detachment system unroofed an infrastructure of high-grade, migmatitic gneiss during Oligocene to early Miocene extension (Dallmeyer and others, 1986; Wright and Snoke, 1993; McGrew and Snee, 1994). Thermobarometric constraints from near the base of the mylonitic zone record deformation conditions of 550°–620°C and 300–400 MPa (Hurlow and others, 1991). Sample WBC6 (143A and 143B) characterizes the mylonitic zone, whereas sample 8706-1 (143C and 143D) is transitional in nature, and sample 8727-3 (143E and 143F) represents the infrastructure (Figure 143.1). These three samples record a decreasing contribution from simple shear strain and an actual reversal in shear sense at the deepest structural levels. Inferred variations in quartz deformation mechanisms probably reflect decreasing strain rate and increasing temperature with depth beneath the detachment. We argue that the East Humboldt Range shear system represents a fundamental boundary between an upper crust deforming primarily by rigid block translation and a deeper crust deforming by regional-scale ductile flow.

143A and 143B These photomicrographs illustrate quartzite from the upper mylonite zone (sample WBC6, at two different scales), <50 m beneath the East Humboldt Range detachment fault, West Fork of Boulder Creek, East Humboldt Range, Nevada. X = lineation, oriented 282°, 5° in geographic coordinates; Y = transverse direction; Z = pole to foliation, oriented 273°, 29°. Mean quartz grain size is approximately 150 μm. Asymmetric mica and feldspar porphyroclasts record WNW-directed (i.e., dextral) shear. Trails of fine, recrystallized muscovite, biotite, quartz, and feldspar define shear planes spaced at 200–1500 μm, and recrystallized quartz shows a weak grain-shape fabric inclined 25°–35° to this spaced foliation, again implying WNW-directed shear (see inset). NX

X-ray texture results (Figure 143.2) show a kinked single girdle of c-axes which is also asymmetric toward the WNW. An extremely strong point maximum of c-axes parallel to Y forms the center of a near-single-crystal preferred orientation, with the dominant a-axis maximum inclined 25° clockwise from X and with the dominant m pole position inclined 5° anticlockwise from X.
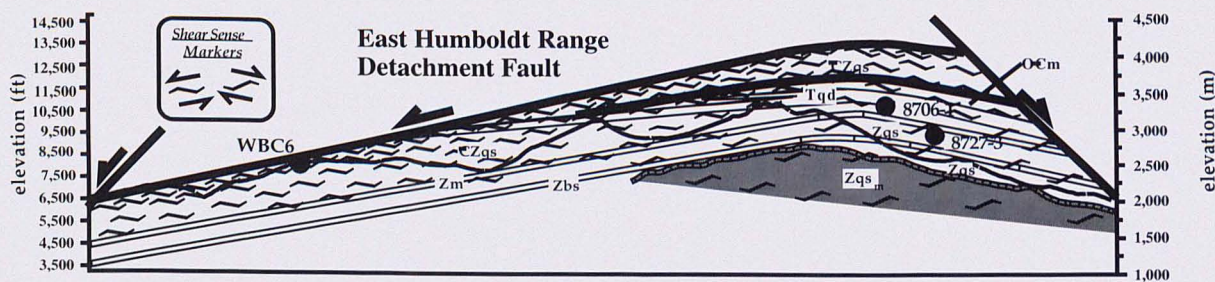

Figure 143.1. Schematic cross section through the central East Humboldt Range, Nevada, showing the structural position of samples relative to the detachment fault. (Note: Sample WBC6 was collected along the line of section but samples 8706-1 and 8727-3 were projected from several kilometers to the north.) Wave pattern indicates shear sense, with closeness of spacing reflecting intensity of deformation.
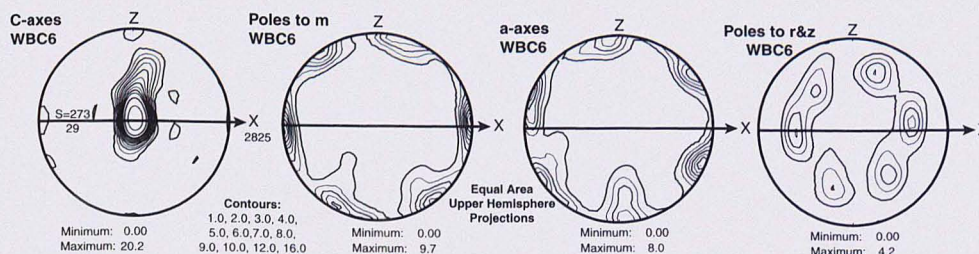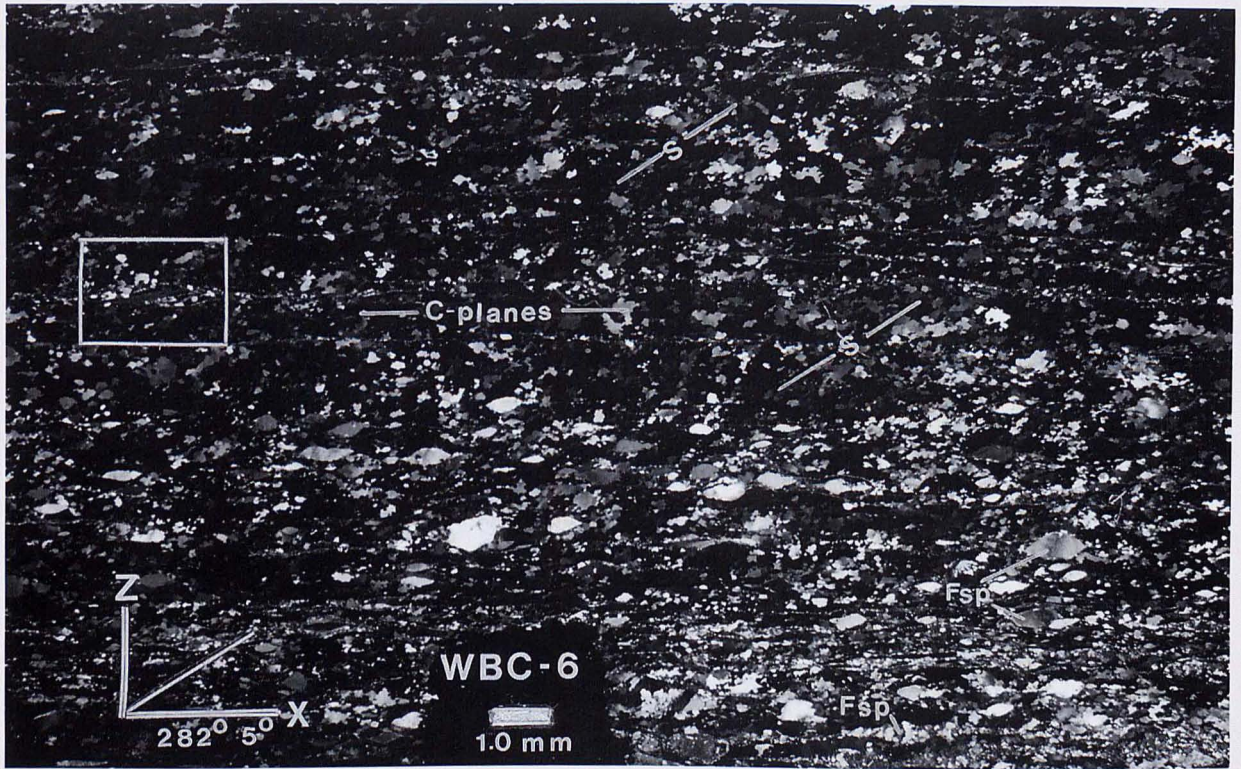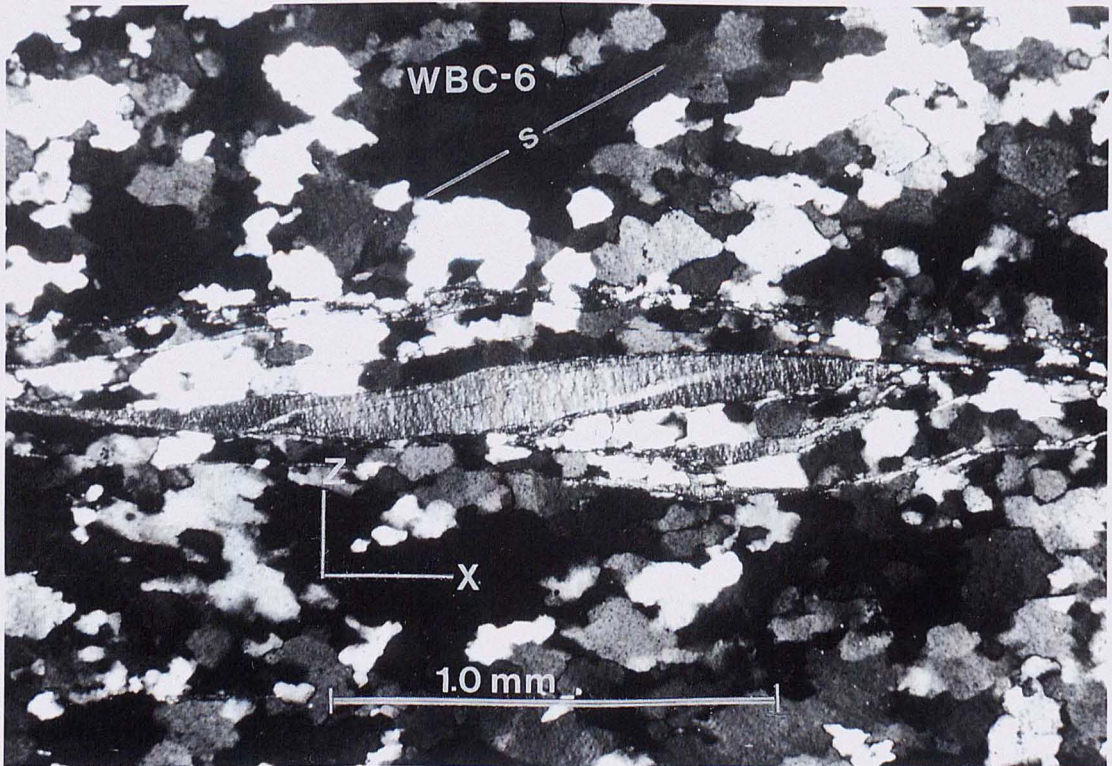

Figure 143.2. Selected pole figures for sample WBC6, regenerated from X-ray data and contoured in multiples of uniform distribution.

143 A

143 B

143C and 143D. These photomicrographs illustrate a gneissic quartzite (sample 8706-1, at two different scales), from the boundary between the mylonitic zone and the infrastructure, approximately 750–1000 m beneath the East Humboldt Range detachment fault, East Humboldt Range, Nevada. The rock is transected by thin seams of fine recrystallized grains spaced at 1000–2500 μm parallel to macroscopic foliation. The mean quartz grain size, in the range 500–700 μm (with very coarse grains >1500 μm), contrasts dramatically with that of sample WBC6 from the upper mylonitic zone (143A and 143B). Subgrains and undulose extinction, though present, are far less common than in the mylonites. Cross-hatched microstructure is common; this consists of interlocking cross-mosaics of quartz grains with crudely rectilinear grain boundaries oriented at moderate angles to bulk foliation, and is characteristic of high-temperature deformation (Lister and Dornsiepen, 1982).

Asymmetric microstructures are virtually absent throughout most of the thin section, but the lower part of the field of view (143C) shows a weak, asymmetric grain-shape fabric defined by elongate grains inclined at 15°–20° to bulk foliation, suggesting domainal WNW-directed, noncoaxial strain, as in the overlying mylonites. Optical inspection shows that this domain is also distinguished crystallographically by a higher proportion of grains with *c*-axes lying in the XZ plane and inclined approximately 45° anticlockwise (i.e., ESE-ward) from X (these grains appear bright in 143C and 143D).

Grains in this orientation have basal planes dipping 45° clockwise from X, thus placing the *c*-axis and the basal plane parallel to the two preferred grain-boundary orientations of the cross-hatched microstructure. NX

Due to the coarse grain size of this sample, X-ray texture data were combined from four separate scans to improve grain-count statistics and to average out domainal variations. The combined X-ray pole figures (Figure 143.3) show an extremely strong *c*-axis maximum oriented subparallel to Y, with little evidence of the subsidiary grain population with *c*-axes oriented in the XZ plane. Although somewhat resembling the strong Y-maximum fabrics from higher structural levels, this texture shows much higher symmetry, particularly evident in the *m*, *a*, and *r* + *z* pole figures.

Grain-boundary migration probably played a pivotal role in the development of both the texture and the microstructure, favoring growth of crystals in preferred orientations, and thus facilitating both the coarse grain size and the strong point maximum texture. The symmetry of the texture suggests a nearly coaxial strain path, with equal resolved shear stresses (and presumably equal activities) on antithetically paired prism ⟨*a*⟩ slip systems. Because macroscopic fabrics are parallel to those from the mylonitic zone, and because nearby Tertiary orthogneisses show similar fabric relationships, we believe that this texture offers a reasonable estimate of the regional background strain path over which mylonitization developed.
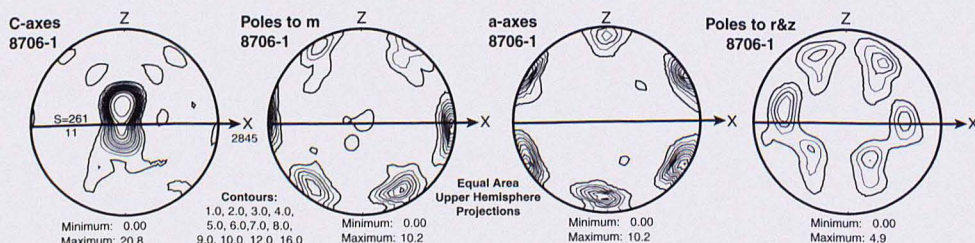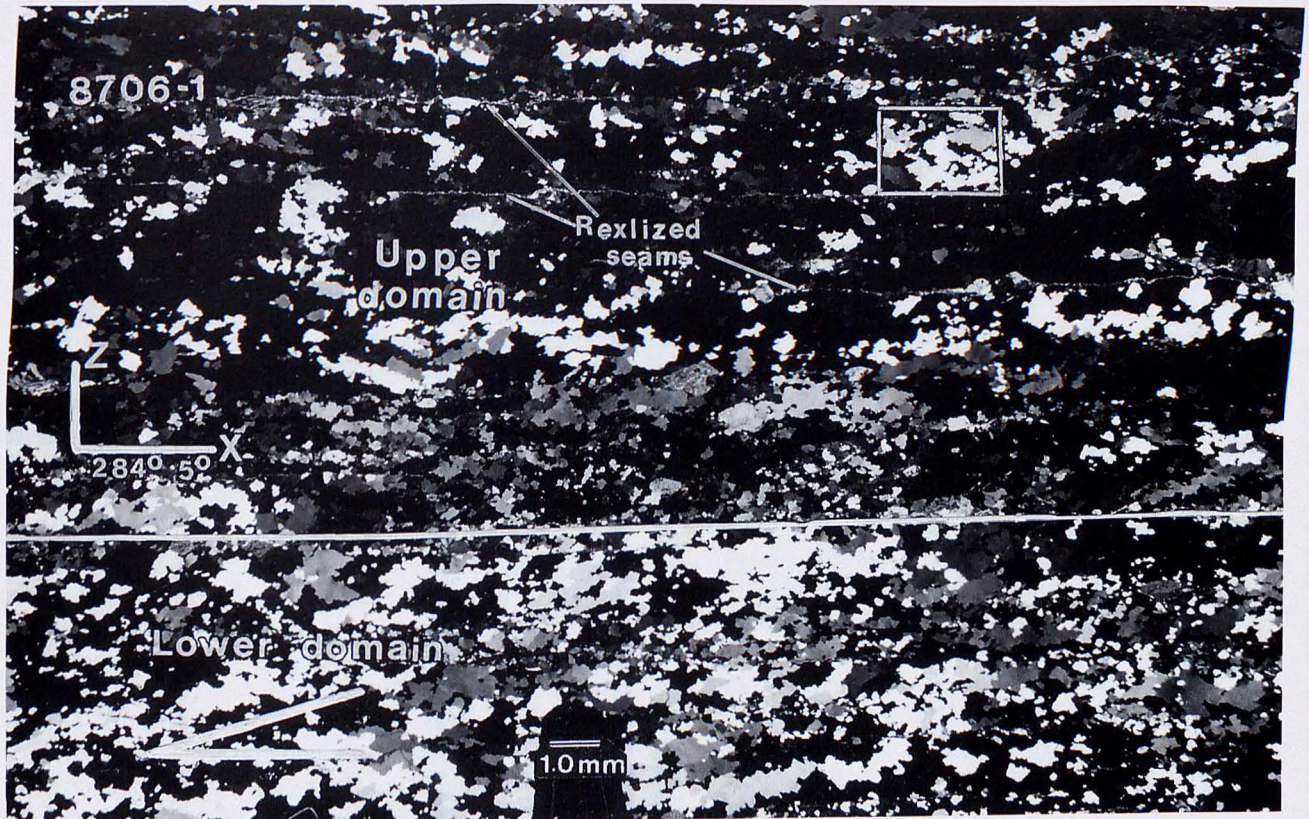

C-axes 8706-1   Z   S=261 11   →X   Minimum: 0.00   Maximum: 20.8

Poles to m 8706-1   Z   2845   Contours: 1.0, 2.0, 3.0, 4.0, 5.0, 6.0, 7.0, 8.0, 9.0, 10.0, 12.0, 16.0   Minimum: 0.00   Maximum: 10.2

a-axes 8706-1   Z   →X   Equal Area Upper Hemisphere Projections   Minimum: 0.00   Maximum: 10.2

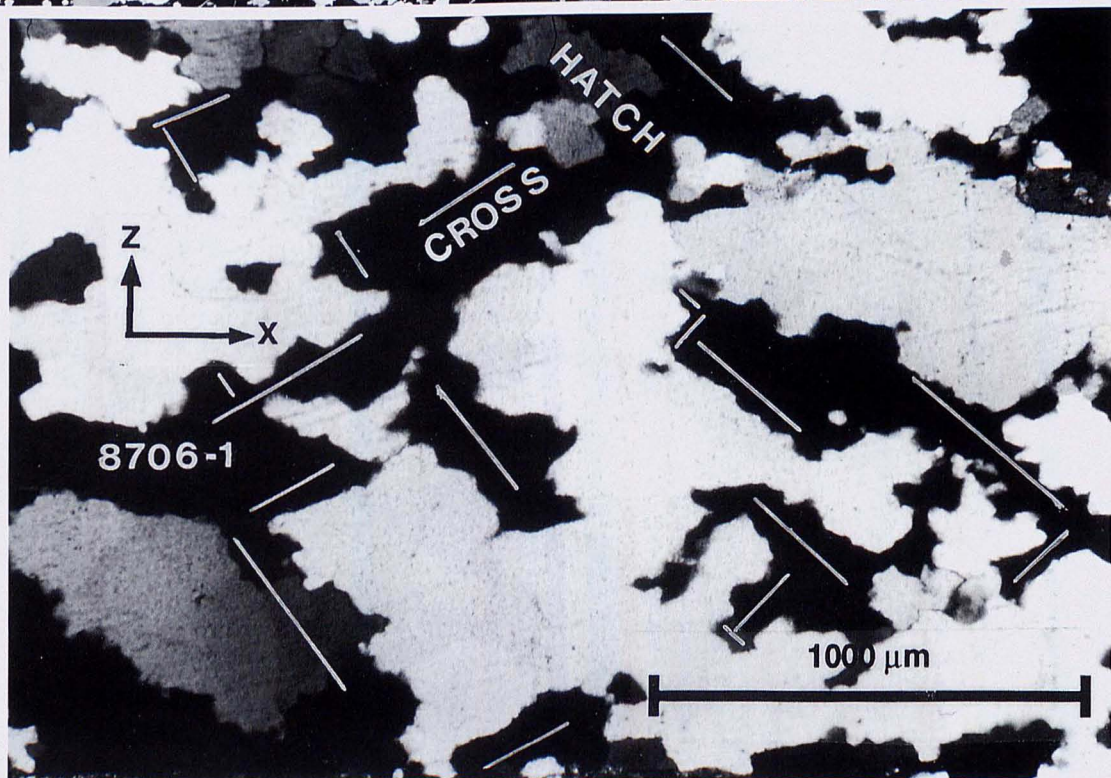Poles to r&z 8706-1   Z   →X   Minimum: 0.00   Maximum: 4.9

Figure 143.3. Selected pole figures for sample 8706-1, regenerated from four X-ray scans and contoured in multiples of uniform distribution.

8706-1

Upper domain

Rexlized seams

Z

X

284° 50

Lower domain

1.0 mm

143 C

HATCH

CROSS

Z

X

8706-1

1000 µm

143 D

143E and 143F. These photomicrographs illustrate a gneissic quartzite (sample 8727-3, at two different scales) from the infrastructure, 1000–1250 m beneath the East Humboldt Range detachment fault, East Humboldt Range, Nevada. Quartz grain size is somewhat domainal in this sample, ranging from approximately 500 μm in the more feldspathic upper domain to >1000 μm in the more biotite-rich, lower domain. Despite the coarse grain size, very fine neoblasts are also present, as are well-developed subgrains, suggesting that the high-temperature deformation characterized by rapid grain-boundary migration was followed by grain-size reduction at lower temperature. Noncoaxial kinematic indicators are uncommon, but some micas show asymmetric shapes, and the more recrystallized upper domain seems to show a subtle quartz grain-shape fabric inclined at 25°–30° to bulk foliation. This suggests weak, domainal noncoaxial strain directed toward the ESE, antithetic to that of the overlying mylonitic zone. Although weakly developed in this sample, ESE-directed kinematic indicators occur locally throughout the infrastructure and suggest a reversal in general shear sense at the deepest structural levels. NX

Due to the coarse grain size of this sample, five X-ray scans were combined to obtain the regenerated pole figures (Figure 143.4), and these agree well with optical results. The crystallographic preferred orientation for this sample consists of three orthogonal maxima, with one maximum near Y and the other two approximately equally inclined to X in or near the XZ plane. Such *c*-axis crystallographic preferred orientations are quite rare and usually occur in granulite-facies terranes (e.g., Lister and Dornsiepen, 1982); complete crystallographic results for such a texture have not been reported previously. The unequal populations of the three maxima impart a weak asymmetry toward the ESE, and the slight misorientation of two of the maxima relative to macroscopic fabric directions imparts a triclinic character to the external symmetry.

An intriguing aspect of these data is the amount of position switching of the *c*-, *m*-, and *a*-axes between the three principal maximum positions. For example, crystals in the central maximum tend to place an *a*-axis and a pole to a first-order prism parallel to each of the other two maxima. Conversely, crystals in the two perimeter maxima tend to place either an *m* pole or an *a*-axis parallel to the other perimeter maximum. Grain-boundary migration probably played an important role in developing this texture by favoring growth of crystals in preferred orientations. If a general, only slightly noncoaxial deformation path is assumed, then *c*-axis positions near Y are well oriented for antithetic slip on paired prism ⟨*a*⟩ systems. Similarly, the *c*-axis maxima positions in the XZ plane are well disposed for paired, antithetic activity on prism ⟨*c*⟩ and basal ⟨*a*⟩ slip systems (Lister and Dornsiepen, 1982). Consequently, we argue for a general, nearly coaxial deformation path with a small contribution from ESE-directed shear.
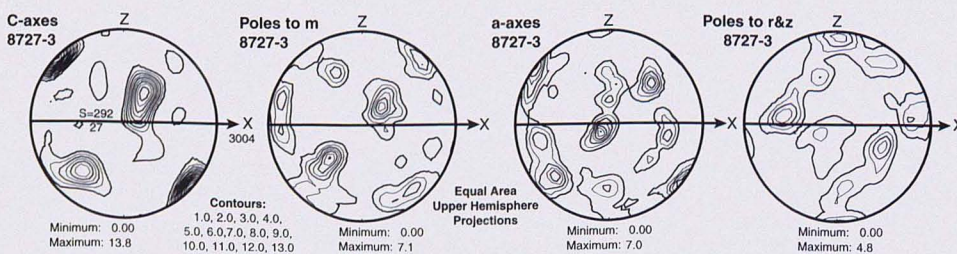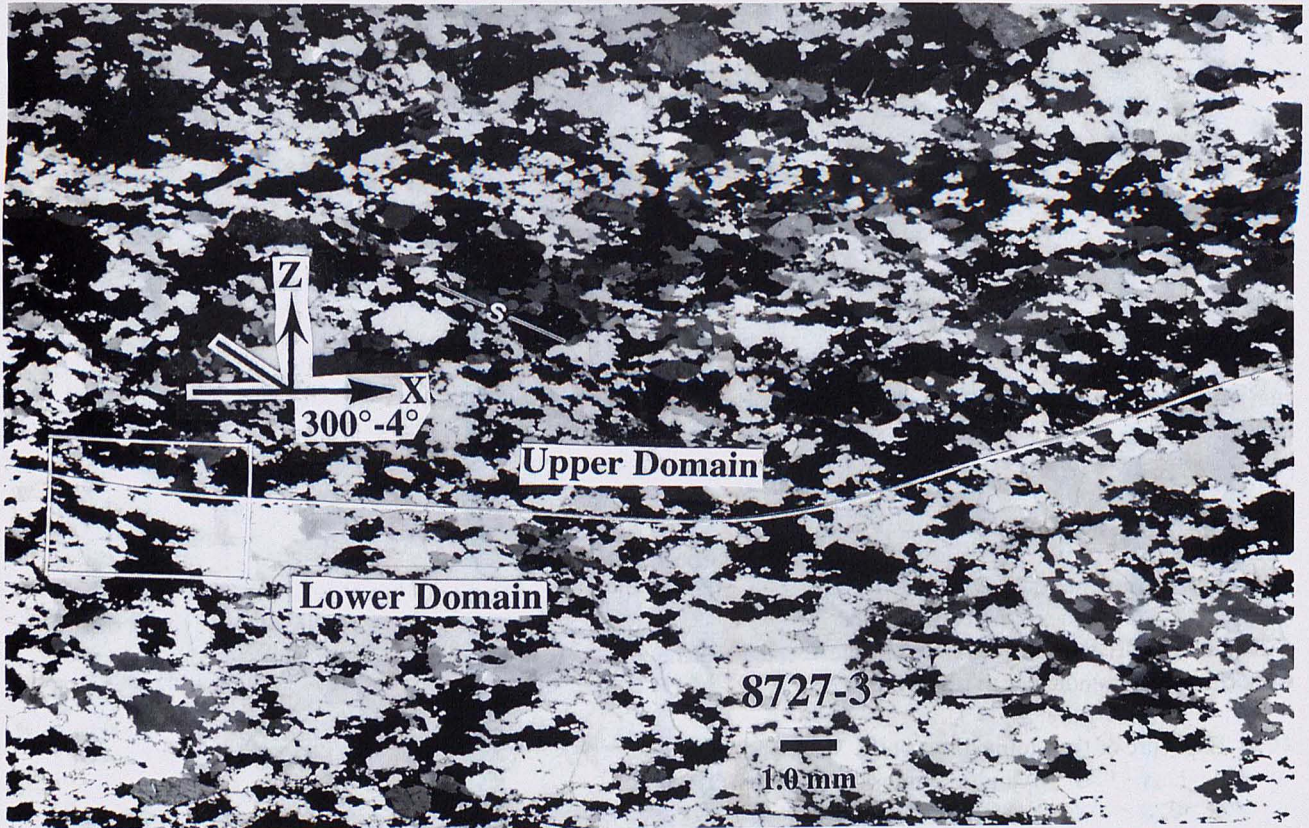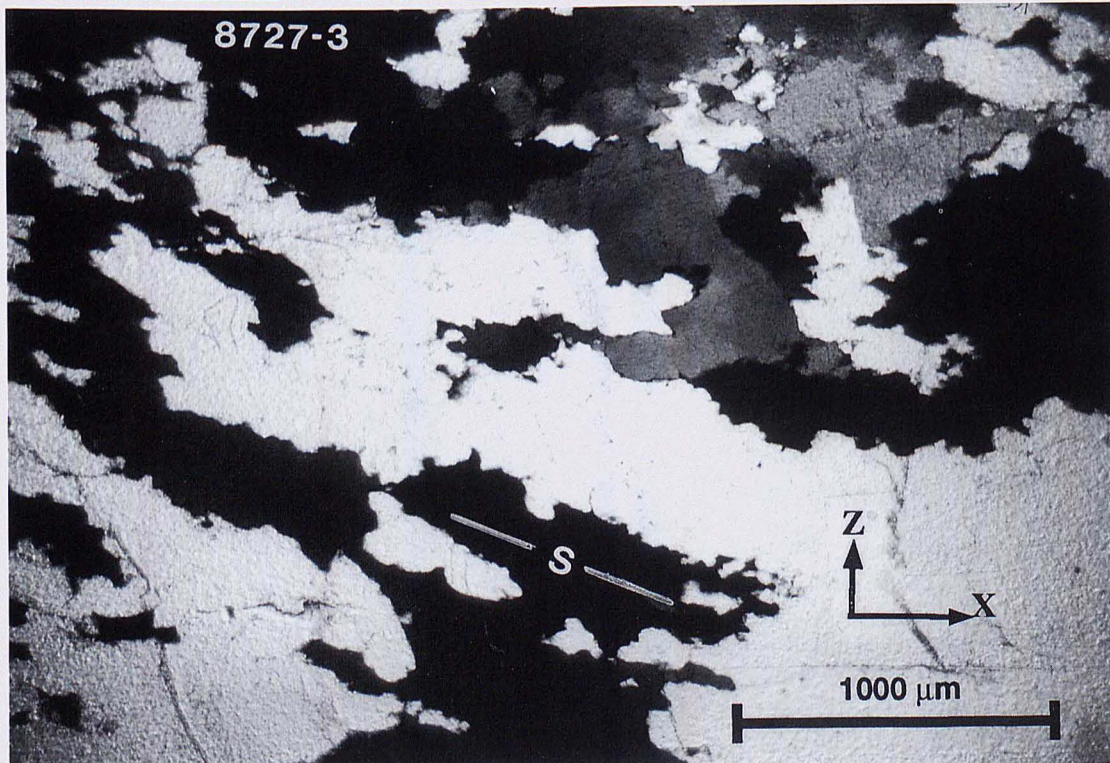

Figure 143.4. Selected pole figures for sample 8727-3, regenerated from five X-ray scans and contoured in multiples of uniform distribution.

Z
300°-4°
X
S
Upper Domain
Lower Domain
8727-3
1.0 mm

143 E

8727-3
S
Z
X
1000 µm

143 F